Toward the systematic investigation of periodic solutions in single reed woodwind instruments

Sami Karkar, Christophe Vergez, Bruno Cochelin

Toward the systematic investigation of periodic solutions in single reed woodwind instruments

Sami Karkar (1,2), Christophe Vergez (1) and Bruno Cochelin (1,3)

(1) Laboratory of Mechanics and Acoustics, UPR 7051 CNRS, Marseille, France
(2) Aix-Marseille University, Marseille, France
(3) Ecole Centrale Marseille, Marseille, France

ABSTRACT

Single reed woodwind instruments rely on the basic principle of a linear acoustic resonator – the air column inside the cylindrical or conical bore, coupled with a nonlinear exciter – namely the reed and the air jet entering the mouthpiece. The first one is described by its input impedance, which binds the acoustical pressure and flow at the entry of the bore through a linear relation, whereas the second one has a non-smooth, nonlinear characteristic which combines the pressure on both sides of the reed channel, the jet flow, and the reed motion. To find possible playing frequencies, one often analyses the input impedance spectrum in terms of central frequency, height and width of peaks – a method used in various recent publications on bore geometry optimisation. The exciter influence has rarely been taken into account, and in a few restrictive cases only : for precise, fixed value of control parameters ; through time domain simulations, which cannot give all information on the dynamics ; through simplifications of the equations, allowing analytical calculations of some parts of the bifurcation diagram. A more systematic investigation of a given instrument behaviors depending on control parameters requires the framework of dynamical systems and bifurcation theory, as well as specific numerical tools. In the present work, two continuation methods were used to obtain the bifurcation diagram of a clarinet, as comprehensive as possible. Stable and unstable, periodic and static solution branches are shown, revealing instrument characteristics such as oscillation, saturation, and extinction thresholds, as well as dynamic range.

INTRODUCTION

In this paper, a method for systematic investigation of static and periodic solutions of single reed woodwind instruments is presented. In the first part, the physical model used for this type of musical instruments is described through a set of nonlinear, non-smooth, ordinary differential equations. Then two numerical methods for continuing fixed points and periodic orbits of a parameter-dependent ODE system are described. In a third part, both tools are applied to the physical model of a clarinet revealing its bifurcation diagram. In the last part, the stable periodic solutions are reviewed in detail and characteristics of the instrument such as oscillation threshold, dynamic range, and playing frequency are extracted.

PHYSICAL MODEL OF SINGLE REED WOODWIND INSTRUMENTS

In this section, the physical model used in this study is presented. The most simple instrument that fits this model is a clarinet with all its holes closed, thus a cylindrical resonator with a single inward-striking reed at its input.

The versatility of this model makes one able to use a measured input impedance of any instrument for realistic modelling. Transposition to the case of lip-reed brass-like instruments as well as double-reed woodwind instruments will demand very little work, as the models are very similar.

Resonator acoustics

Let us consider the pressure P and the flow U at the input of the resonator. We use the decomposition of the input impedance

Figure 1: Schematics of the clarinet and variables used in the physical model.

into complex modes proposed in [11] which leads to the following general form :

$$Z_{in}(\omega) = \sum_{n=1}^{N_m} \left(\frac{C_n}{j\omega - s_n} + \frac{C_n^*}{j\omega - s_n^*} \right) \quad (1)$$

where N_m is the number of modes taken into account, s_n are the poles of impedance and C_n their corresponding residues.

Remarks :

- whether using an analytical or a measured input impedance, either poles and residues numerical determination or curve fitting is needed to obtain the values of the coefficients s_n and C_n ;
- $\mathscr{I}m(s_n)$ gives the angular frequency of the nth mode, $\mathscr{R}e(s_n)$ its damping, and $|C_n|/\mathscr{R}e(s_n)$ the amplitude of the corresponding peak of the impedance spectrum ;
- N_m is typically between 10 and 20, because either the cut-off frequency of the tone-hole lattice or the reed low-pass filter behaviour makes high frequency modes useless ;

- the input impedance written as above is not equal to zero at null frequency, as it is usually the case, but has a modulus of the same order of magnitude as those of the lowest minima of the impedance spectrum. Even though the resistance of the bore to a constant flow should be derived from fluid dynamics, the impedance induced by a stationary flow is much lower than usual acoustical impedances, and the approximation should be valid.

Reed motion

The motion of the reed tip $h(t)$ is driven by the pressure in the mouth of the player P_m (a constant or slowly varying parameter) on one side and the pressure at the input end of the bore $P(t)$ on the other side (see schematics on fig. 1 and 2) through a single mode mechanical equation :

$$\frac{1}{\omega_r^2}h''(t) + \frac{q_r}{\omega_r}h'(t) + (h(t)-h_0) = \frac{P(t)-P_m}{K} \quad (2)$$

where ω_r and q_r are the angular frequency and damping parameters of the reed, which may vary depending on the player's control of the embouchure, and K is the equivalent stiffness of the reed.

Introducing the characteristic pressure $P_c = Kh_0$ (which represents the minimum static pressure difference needed to close the reed channel), and the dimensionless variables $x = h/h_0$, $y = x'/\omega_r$, $p = P/P_c$ and $\gamma = P_m/P_c$, a dimensionless form of the previous equation is :

$$y'/\omega_r = 1 - x + p - \gamma - q_r y. \quad (3)$$

Moreover, the reed tip position is limited by a unilateral contact with the mouthpiece, which means $x(t) \geq 0$ at all times. As we will see later, it is quite difficult to solve numerically this kind of non-smooth contact law and the adopted regularisation sometimes let x be slightly negative.
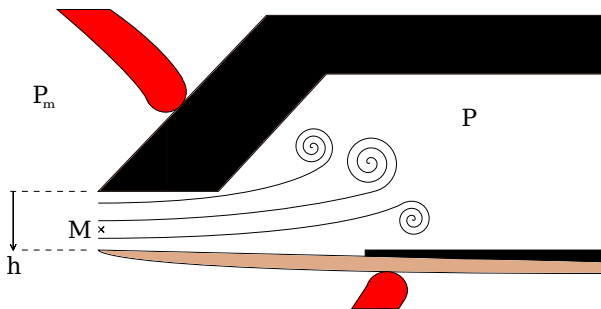

Figure 2: Schematics of the mouthpiece showing how the flow expression is derived from the Bernoulli theorem.

Flow through the reed channel

As carefully explained in [6, 11], the application of Bernoulli theorem between a remote point in the mouth of the player with pressure P_m and velocity v_m and a point M of the same field line in the reed channel (see fig. 2) with pressure P_{rc} and velocity v_{rc} leads to the following equation :

$$\rho\frac{v_m^2}{2} + P_m = \rho\frac{v_{rc}^2}{2} + P_{rc}. \quad (4)$$

Assuming a constant velocity profile in the reed channel (this is obviously not true, but will lead to a mean velocity), the flow U is simply v_{rc} multiplied by the reed tip opening $h(t)$ and the reed channel width W. Let us now neglect v_m because $|v_m| << |v_{rc}|$. Assuming that the jet formed at the output of the reed channel is totally dissipated by turbulence (without

pressure recovery, so that $P = P_{rc}$) and using conservation of the flow, one gets to :

$$U(t) = Wh(t)\sqrt{2\Delta P/\rho} \quad (5)$$

where $\Delta P = P_m - P(t)$ is the pressure difference between the mouth of the player and inside the mouthpiece.

In the case where $\Delta P < 0$, the problem is almost symmetrical and the same considerations leads to :

$$U(t) = -Wh(t)\sqrt{-2\Delta P/\rho} \quad (6)$$

Let us point out that this case has to be included because ΔP might become negative with $h > 0$.

Using the characteristic flow $U_0 = Wh_0\sqrt{2P_M/\rho}$, we define the dimensionless flow $u = U/U_0$ and get the following unique dimensionless form :

$$u(t) = \mathrm{H}(x(t))\mathrm{sign}(\gamma-p(t))x(t)\sqrt{|\gamma-p(t)|} \quad (7)$$

where the Heaviside function has been added to deal with any possible negative x value (which, let us recall, might happen when solved numerically because of the regularisation of the non-smooth unilateral contact condition, but is not physical).

Pressure-flow equation

Back to the time domain, the input impedance presented above leads to the following relationship between the flow U, the pressure P and its modal components P_n :

$$P_n'(t) = C_n U(t) + s_n P_n(t) \quad (\text{for } n = 1..N_m) \quad (8)$$

$$P(t) = 2\sum_{n=1}^{N_m} \mathscr{R}e(P_n(t)). \quad (9)$$

As previously, we define the dimensionless variables $p_n = P_n/P_M$ and get to the following dimensionless equation :

$$p_n'(t) = U_0/P_M C_n u(t) + s_n p_n(t) \quad (\text{for } n = 1..N_m) \quad (10)$$

$$p(t) = 2\sum_{n=1}^{N_m} \mathscr{R}e(p_n(t)). \quad (11)$$

FRAMEWORK : SOLUTIONS OF A DYNAMICAL SYSTEM AND THEIR CONTINUATION

In this section, we recall a few basic definitions and results concerning dynamical systems, which will be useful when dealing with the numerical methods.

We consider a physical system that is described by an (a set of) ordinary differential equation(s) of the general form :

$$x' = f(x,\lambda) \quad (12)$$

where $x(t)$ is the state vector of the system, $x'(t)$ its time derivative, and λ some parameter that might have influence on the trajectories.

Continuation of fixed-points and periodic solutions

A fixed point of such a system is a particular solution of (12) that does not vary in time. Thus it is solution of the algebraic equation :

$$f(x,\lambda) = 0 \quad (13)$$

Knowing a fixed point (x_0, λ_0), there exists (under some conditions on f) a continuum of similar solutions $(x(\lambda), \lambda)$ in a neighbourhood around λ_0. Investigating the influence of the parameter on the given solution is called the continuation (or

path following) of a fixed-point solution and consists in calculating the *branch* formed by these continua.

A periodic orbit of the considered system is a periodic function of the time $x : t \rightarrow x(t)$, of shortest period T, that is solution of (12) at all times. In case of a periodic orbit, the same kind of results exists and allows the continuation a given periodic solution along a branch when the parameter is varied.

METHODS : NUMERICAL TOOLS FOR CONTINUATION

Whereas linear dynamical systems may be investigated analytically, non-linear and moreover non-smooth systems are often difficult to study without numerical tools. Time integration or simulation tools are one of the possible ways of dealing with the difficulty. However, it usually does not uncover all solutions of a given system, especially unstable solutions. Thus, numerical continuation tools are useful to investigate the general behaviour of a system.

Numerical tools are usually designed to solve algebraic equations and continue their solutions. It is thus straightforward to compute branches of fixed-points, whereas for continuing periodic orbits, a discretization is necessary to come down to an algebraic system. Two approaches are then possible :

- Time-domain discretization consists of sampling the solution $x(t)$ over one period into a set of discrete values $\{x(t_0), x(t_1), ..., x(t_N = t_0 + T) = x(t_0)\}$. The problem is then solved for each time sample using a dedicated method like collocation or differentiation scheme, leading to an algebraic problem.
- Frequency-domain discretization is made possible by the Fourier representation of a periodic function. The harmonic balance method then leads to a set of algebraic equations.

Prediction-Correction Method

A classical Prediction-Correction Method (or PCM) consists of two steps. Starting from a given solution x_i for the value λ_i of the parameter and the quantity $\dot{x}_i = \frac{dx}{d\lambda}\big|_{(x_i, \lambda_i)}$ (which is the tangent of the curve representing the solution branch in a λ-x plane), the prediction step is the computation of a rough approximation of the solution $x_{i+1}^0 = x_i + \Delta\lambda \dot{x}_i$ for the value of the parameter $\lambda_{i+1} = \lambda_i + \Delta\lambda$ (see figure 3). Then an iterative correction algorithm is used to get a better approximation of the solution (at numerical precision).
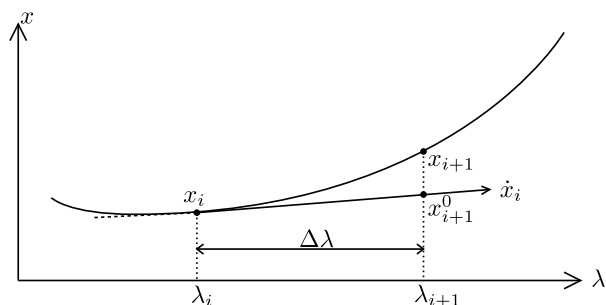

Figure 3: Illustration of the tangent predictor.

In the software AUTO [5] that was used in this study, a specific parametrisation of the curve called pseudo arc-length is used (see [7]), allowing to proceed with the continuation even through points where the "tangent", as defined above, tends to infinity (limit points). As this introduces a new variable into the

system, namely the pseudo arc-length parameter, a new equation is needed. It is brought by the parametrisation equation, which locally defines this new variable : $s = (x(s) - x_i).x_i^t + (\lambda(s) - \lambda_i).\lambda_i^t$ where the superscript t refers to the (newly defined) tangent. In this case, defining the length of the step as Δs, the tangent predictor is :

$$x_{i+1}^0 = x_i + \Delta s x_i^t \tag{14}$$

$$\lambda_{i+1}^0 = \lambda_i + \Delta s \lambda_i^t. \tag{15}$$

The correction step then uses a Newton-Chord algorithm to converge to the next solution (x_{i+1}, λ_{i+1}).

Asymptotic Numerical Method

The MANLAB software (available online, see [8]), also used in this study, relies on the Asymptotic Numerical Method (or ANM). Its basic principle is a local high-order Taylor series expansion of all quantities as functions of a path parameter s, which is also the pseudo arc-length parameter in this case. Letting (x_i, λ_i) be a known solution of (13) for $(x(s), \lambda(s))$ to lie on the solution branch for all s in some interval $[0, s_{max}]$, we write :

$$x(s) = x_i + \sum_{n=1}^{+\infty} s^n x_i^{(n)} \tag{16}$$

$$\lambda(s) = \lambda_i + \sum_{n=1}^{+\infty} s^n \lambda_i^{(n)}. \tag{17}$$

Then the $x_i^{(n)}$ and $\lambda_i^{(n)}$ are solutions of a new system of recursive linear equations with invariant left-hand side matrix. Truncating the series to a high order N (typically 15 to 30) gives an accurate, smooth, and continuous description of the branch for values of s below the convergence radius of the series. This way, one can compute a continuous portion of the branch of length s_{max}, which is determined a posteriori as the value of s for which $|f(x(s), \lambda(s))|$ reaches a user-defined tolerance threshold. A piecewise-continuous representation of a whole branch of solutions is thus obtained by connecting several portions of the branch.

Notes :

- fixing $N = 1$ is equivalent to the tangent predictor of the previous method with $x_i^1 = x_i^t$, thus the ANM can be considered as a high-order prediction method ;
- a classical Newton-Raphson algorithm has been implemented in case residues would accumulate through steps, but experience shows that usually no correction is needed.

Periodic solutions continuation

Concerning the first method (PCM), the AUTO software uses orthogonal collocation for the continuation of periodic orbits (see [5, 4] for details). The periodic solution is sampled over a period using piecewise polynomial interpolation on each time interval. Writing (12) for each collocation point leads to a system of algebraic equations. The solution of this system are then continued with the PCM. The number of time intervals for the discretization of the period is adjustable, as well as the number of collocation points per time interval, which defines the order of the interpolation.

In the MANLAB software, the investigation of periodic solutions is carried out combining the Harmonic Balance Method and the ANM. As a periodic solution is described with its truncated Fourier series, the HBM links the coefficients of this series and the angular frequency ω through a system of algebraic

equations derived from the primary system (12) using trigonometric identities. The ANM is then used for continuing the solutions of this new system. The reader is refered to [2] for a detailed description and practical application.

Remark : fixing $\omega = 0$ as the phase equation of the HBM allows to compute static solutions (fixed-points).

RESULTS AND DISCUSSION

In this section, both methods are applied to the physical model of clarinet described in the first section. As we are interested in what happens when the player's blowing pressure varies, γ is chosen as the continuation parameter.

The static solution branch as well as several periodic solution branches, rising from direct Andronov-Hopf bifurcations of the static branch, are obtained. Stability analysis is performed and the only stable periodic regime is reviewed in details.

The values used for the parameters of the model are shown in table 1. The modal coefficients C_n and s_n are the poles and residues of the analytical input impedance for a cylinder of length L and radius r, determined using the MOREESC software (see [11, 9]). Visco-thermal losses are taken into account, but not radiation.

Table 1: Model parameters for a clarinet-like instrument

L	r	N_m	W	h_0
650 mm	7 mm	12	12 mm	.3 mm

$\omega_r/2\pi$	q_r	K	ρ
1500 Hz	1	8.10^6 Pa/m	$1,185$ kg/m^3

Static regime of the clarinet

In the static case (i.e. fixed-point solutions), the branch can be computed analytically as the solution of a third degree polynomial equation. The solution branch computed by both softwares are perfectly superimposed on each other and on the exact solution (up to numerical precision). However, the use of the AUTO software is preferred here since it performs a stability analysis and detects Andronov-Hopf bifurcations. The result is shown figure 4. The trivial solution where all quanti-
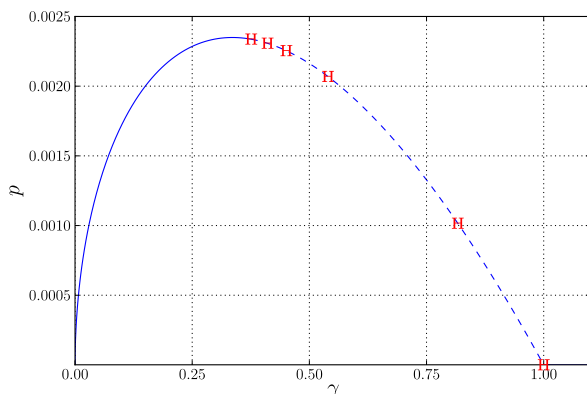

Figure 4: The static regime of the clarinet.
— : stable parts - - : unstable parts
H : Andronov-Hopf bifurcation.

ties are null for $\gamma = 0$ being a singular point (the jacobian of the system is not invertible), it cannot be used as a starting point for continuation. An analytical solution for $0 < \gamma < 1$ has been used instead.

Several bifurcation points appear. All of them are of the Andronov-Hopf type, and a periodic solution branch rises from each one of them. As it will be shown further, the position of the first bifurcation gives the value of γ that is commonly referred to as the oscillation threshold.
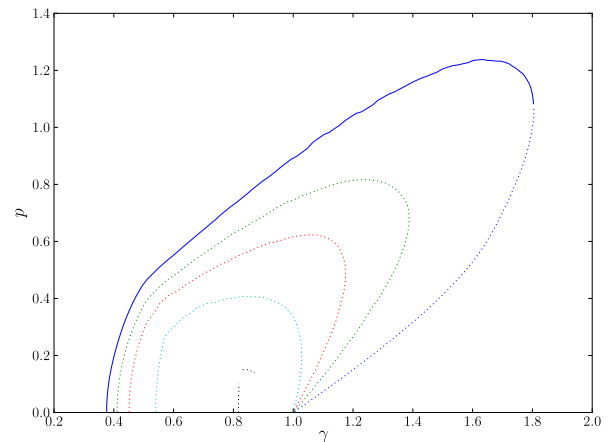
Bifurcation diagram

Figure 5: Bifurcation diagram of the clarinet computed with AUTO. R.-m.-s. value of p vs γ. Plain line : stable parts ; dotted lines : unstable parts. The static branch is not visible at this scale.

The computation of these periodic regimes has been carried out. Figure 5 shows the bifurcation diagram of our model : the root-mean-square value of p (computed over one period) is plotted versus γ for each periodic branch computed with AUTO.

Some branches are quite difficult to compute and a refined mesh of the period is needed to achieve convergence. The fifth branch is problematic, despite a very fine mesh and very small steps. Thus, the bifurcation diagram displayed here is slightly incomplete. However, it must be noticed that only the first periodic regime is stable, and other branches have less physical interest. Another important remark is that the first Andronov-Hopf bifurcation (which is the oscillation threshold) is direct in our case. An extended exploration of the parameter space (especially ω_r and q_r that can vary through the control of the embouchure by the player) within realistic ranges would be very interesting, to see if an inverse bifurcation is possible at the oscillation threshold with this model (as shown in [12] and [11]).

Remark : the extinction is a discontinuity-induced, degenerate bifurcation as all periodic branches converge towards the same point in $\gamma = 1$, with non-vertical tangents.

Stable periodic regime : details

As it has been pointed out, only the first periodic regime is stable in our case, and thus of great interest. Figure 6 shows this first periodic regime, computed with MANLAB. Root-mean-square as well as maximum value of p over one period (which represents the envelope of the periodic orbits) are plotted versus γ.

The branch differs slightly from the first one computed with AUTO in two regions : near saturation the branch seems to "oscillate" ; near the inverse bifurcation at extinction, the branch is not straight and does not converge to $\gamma = 1$. The first phenomenon is mainly caused by the Fourier truncation : in this
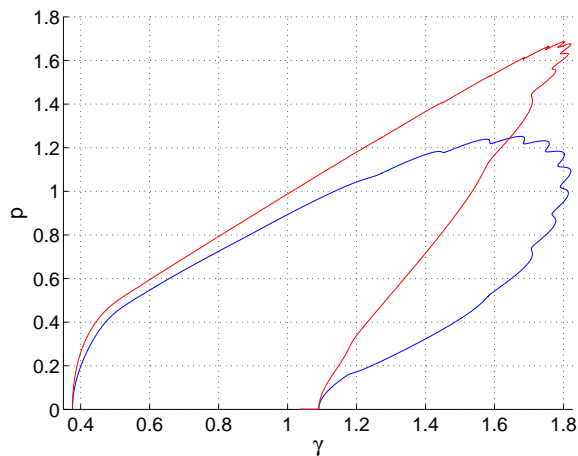
Figure 6:　First periodic regime of the clarinet computed with MANLAB. — : rms value of p, — : max value of p.

Figure 7:　Variation of the fundamental frequency f_0 along the stable part of the periodic regime.

region, the x time-domain solutions are close to square signals, thus the truncation of Fourier series is critical. While with 15 harmonics there were large oscillations, the results of figure 6 is computed with 25 harmonics and only exhibits little oscillations. The second phenomenon is due to the regularisation of the unilateral contact force in the mechanical equation. In MANLAB, the force is written in the form : $F_{reg} = \varepsilon/x^2$ with $\varepsilon << 1$. Thus, in the region where x tends to 0 because of a high pressure difference, the regularisation introduces significant relative errors. A smaller regularisation parameter ε makes the branch to vanish closer to $\gamma = 1$, but makes the problem stiffer, thus leading to smaller steps and demanding a higher H to obtain convergence.

The lowest value for γ of this branch gives the oscillation threshold : $\gamma_{osc} = 0,376$. By monitoring the harmonics of the x part of the solution, one can deduce the threshold of beating reed : $\gamma_{br} = 0,498$. The highest point on the r.-m.-s. value curve gives the saturation threshold : $\gamma_{sat} = 1,63$, which is related to the dynamic range as it is the loudest possible sound : $p_{max} = 1,237$. The rightmost point of the curve gives the extinction threshold (for increasing blowing pressure) : $\gamma_{ext} = 1,805$, beyond which the reed is stuck against the mouthpiece and thus $p = u = x = 0$.

Remarks :

- all parameters other than γ have fixed values, so it does not represent the general dynamic range of the clarinet, but rather a theoretical one, for this set of parameters ;
- experimental data are usually displayed in a way that shows only the envelope of the periodic orbits, which would here correspond to the red curve. However, the loudest sound that can be produced corresponds to the maximum of the r.-m.-s. value of p, which differs in our case from the maximum of its envelope because the signals are neither sinusoidal nor square and their harmonic content varies along the branch. Thus the dynamic range should be deduced from the blue curve ;
- the extinction is an inverse bifurcation as there exists two stable regimes (one periodic, one static) for $1 \leq \gamma \leq \gamma_{ext}$, exhibiting a hysteretic behaviour : the extinction threshold for increasing γ and the oscillation threshold for decreasing γ are different.
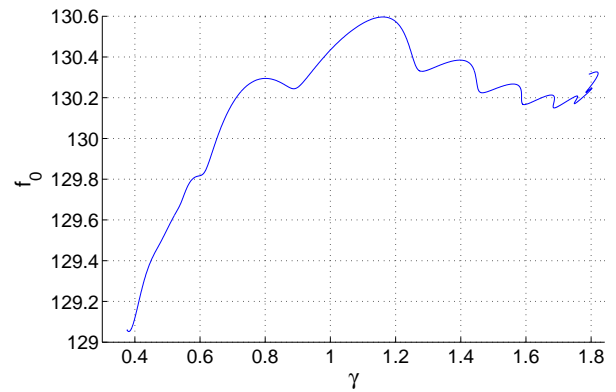
Frequency-domain features

A lot of frequency-domain related quantities are directly accessible along the branch. For instance, we plotted the playing frequency as a function of γ on the figure 7. It shows that the fundamental frequency variation amplitude is up to 18 cents, which is more than noticeable for any normal listener. Thus, the player will be forced to modify other parameters such as the reed's initial opening, or natural frequency and damping, using his lips, to keep the pitch as correct as possible while playing louder. Also, despite the oscillations visible at the end of the branch (causes have been discussed previously), there is a noticeable decrease of the playing frequency when γ is increased from $1,1$ to $1,7$. The playing frequency must be compared with the first resonance frequency of the pipe : $\mathscr{I}m(s_1)/2\pi = 130,44$Hz.

This frequency is actually not representative of a real Bb clarinet : 65cm represents the total length, including the bell, whereas the effective length to consider turns out to be closer to 57cm. However, let us recall that it is only a parameter of the model that has been arbitrarily chosen. As the general behaviour is not sensibly affected, and as the main purpose of this paper is to present a new tool of investigation, all the results presented here are still valid. As for the results concerning a real clarinet, a measured impedance of the instrument would be better, and a precise identification of the reed's parameters would be necessary (which appears not to be simple, according to recent experiments on artificial mouth related in [11]).

Another interesting point is to investigate Worman's rule [13]. Using the representation adopted in previous studies (see [1, 3], the figure 8 shows the odd harmonics (1, 3, 5, 7, and 9) as functions of the first harmonic in logarithmic scale. Straight lines with respective slopes 1, 3, 5, 7 and 9 are plotted for comparison.

The result is in good agreement with Worman's modified rule (given and demonstrated in Ricaud [10]) $P_n = \alpha_n(\gamma - \gamma_{osc})^{n/2}$ where the constant α_n is different for each harmonic. However, it is very important to link this figure to the whole branch of solution : the agreement is only good until $P_1 = -12$dB, which correspond to $\gamma = 0,379$. Going back to figure 6, one can see how narrow is the range of γ, from the oscillation threshold $(0,376)$ to this value. This results indicate that, despite the argument given by Benade in [1], the so-called "change of feel", characterised by a change of slope of the curves $P_n = f(P_1)$, is not due to the reed beating against the mouthpiece : the beating reed threshold ($\gamma_{br} = 0,498$) lies far beyond the limit of
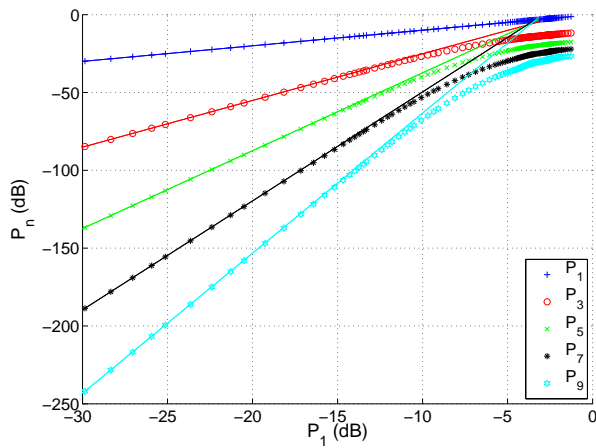
Figure 8: Amplitude (log. scale) of odd harmonics P_n as functions of the first one P_1. Straight lines correspond to slope 3, 5, 7, and 9.

this range.

The advantage of using the HBM with MANLAB is that one have a direct access to the amplitude of the harmonics. It is then very easy to plot the amplitude evolution of each (odd) harmonic with γ as shown on figure 9. It reveals that for the main part of the branch, the relative amplitude of each odd harmonic with respect to the first one is almost constant : $P_1 - P_3 \simeq 10$dB, $P_1 - P_5 \simeq 16$dB, $P_1 - P_7 \simeq 21$dB, and $P_1 - P_9 \simeq 25$dB.
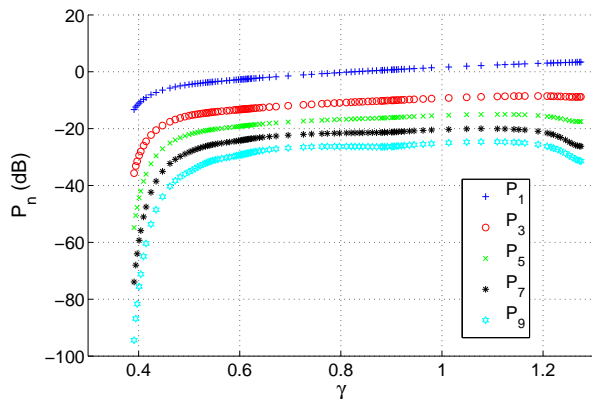

Figure 9: Amplitudes (log. scale) of odd harmonics as functions of γ.

Time-domain point of view

Reconstructing the time series for variables of interest (the internal pressure p, the flow u, and the reed tip position x) is also possible, demands little post-processing, and can be displayed for any point on the branch. Figure 10 shows such time-domain views for $\gamma = 1, 80$, just before extinction. As it can be seen, the reed channel is closed during 70 percents of the period, resulting in a null flow in the mean time. Though, little oscillations of x and u around 0 are visible. It is the result of the Fourier truncation (here $H = 25$) which is not high enough to render correctly tangent discontinuities.
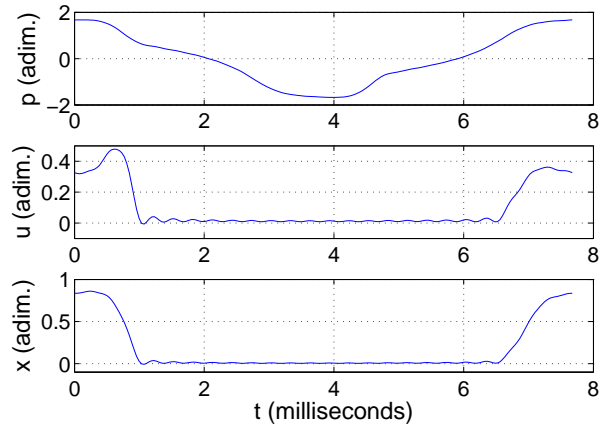

Figure 10: Reconstructed time series for p, u and x just before exctinction.

CONCLUSIONS AND PROSPECTS

As analytical expressions for input impedance of various resonator are often available, allowing to compute easily resonance frequency, analytical work becomes very difficult to apply when one considers the whole dynamical system, especially in the case of highly non-smooth interaction like unilateral contact or dry friction. Then, numerical methods are useful for accessing all characteristics of a given model without simplification or restriction on the parameter values.

In this paper, a physical model for single-reed woodwind instruments has been presented. The static as well as periodic solutions of a clarinet-like instrument based on this model have been investigated. A classical numerical tool for bifurcation analysis, the AUTO software, has been used for the continuation of static branches and bifurcation detection, as well as periodic orbits continuation. A new tool based on the Asymptotic Numerical Method and a high-order harmonic balance formulation, the MANLAB software, has been presented and used for periodic solution continuation.

Lots of characteristics are accessible through the computation of the bifurcation diagram, which reveals the general behaviour of the studied instrument. This tool can also be used as a powerful method for comparison between models, and quantifying the influence of approximations.

In future works, the method will also be applied to the saxophone. Measured input impedance spectrum of real instruments will be used, allowing comparison with artificial mouth experimental data. An adaptation to the (very similar) physical model of brass-like instruments is in progress. Comparison with experiments is necessary and parameter identification would be very interesting. Also, specific path following methods will be applied for the continuation of special points (bifurcations, extrema, ...) with respect to a second parameter.

New developments allowing the investigation of quasi-periodic solutions are also considered.

THANKS

REFERENCES

[1] Arthur H. Benade. "Fundamentals of Musical Acoustics". New-York: Oxford University Press, 1976. Chap. The Woodwinds: I, pp. 430–464.

[2] Bruno Cochelin and Christophe Vergez. "A high order purely frequency-based harmonic balance formulation for continuation of periodic solutions". *Journal of Sound and Vibration* 324 (2009), pp. 243–262.

[3] Jean-Pierre Dalmont et al. "Some Aspects of Tuning and Clean Intonation in Reed Instruments". *Applied Acoustics* 46 (1995), pp. 19–60.

[4] C. De Boor and B. Swartz. "Collocation at gaussian points". *SIAM J. Numer. Anal.* 10.4 (Sept. 1973).

[5] E. J. Doedel and B. E. Oldeman. *AUTO-07P : Continuation and Bifurcation Software for Ordinary Differential Equations*. Concordia University. Montreal, Canada 2009.

[6] A. Hirschberg. "Mechanics of Musical Instruments". CISM Courses and Lectures 355. Wien - New York: Springer, 1995. Chap. 7, pp. 291–369.

[7] H. B. Keller. "Numerical Solution of Bifurcation and Nonlinear Eignevalue Problems". *Applications of Bifurcation Theory*. Academic Press, 1977, pp. 359–384.

[8] *MANLAB, an interactive continuation software*. http://manlab.lma.cnrs-mrs.fr.

[9] *MOREESC, Modal Resonator-Reed Interaction Simulation Code*. http://moreesc.lma.cnrs-mrs.fr.

[10] Benjamin Ricaud et al. "Behavior of reed woodwind instruments around the oscillation threshold". *Acta Acustica* 95.4 (2009), pp. 733–743.

[11] Fabrice Silva. "Emergence des auto-oscillations dans un instrument de musique à anche simple". PhD thesis. Univ. de Provence, LMA - CNRS, 2009.

[12] Fabrice Silva et al. "Interaction of reed and acoustic resonator in clarinet-like systems". *Journal of the Acoustical Society of America* 124.5 (Nov. 2008), pp. 3284–3295.

[13] Walter Elliott Worman. "Self-sustained nonlinear oscillations of medium amplitude in clarinet-like systems". PhD thesis. Case Western Reserve University, 1971.